SEM-BASED MORPHOLOGICAL ANALYSIS OF THE NEW GENERATION AION-BASED ABRASIVE GRAINS (Abral®) WITH REFERENCE TO Al_2O_3/SiC/cBN ABRASIVES

K. Nadolny*, W. Kapłonek

Department of Production Engineering, Faculty of Mechanical Engineering,
Koszalin University of Technology, Koszalin, Poland.

*Corresponding author, E-mail: krzysztof.nadolny@tu.koszalin.pl, phone: +48 94 3478412.

Recibido: Noviembre 2014. Aprobado: Enero 2015.
Publicado: Mayo 2015.

ABSTRACT
This paper presents the general characteristics of a new generation of abrasive grains made from alumina oxynitride AlON manufactured under the trademark Abral®. The chemical composition and main characteristics of these grains were given in relation to the most popular abrasive materials, such as: white fused alumina 99A, microcrystalline sintered corundum (SG^{TM}), green silicon carbide 99C, and mono- and microcrystalline cubic boron nitride (cBN). Within the section that covers the experiment the methodology of micrograph acquisition, using scanning electron microscopy (SEM) techniques, was described in detail, as well as its processing methodology and analysis, which was conducted in order to obtain information about the morphological characteristics of the evaluated abrasive grains. The data obtained is presented in the form of a representative set of SEM micrographs registered for the six variations of the abrasive grains, together with an analysis of the differences in their morphology. As a result of the experimental investigations it was found that the Abral® grains are very similar to white fused alumina 99A grains, in terms of features such as: polycrystalline structure, pointed shape, developed surface and values of apex angles.

Keywords: SEM micrograph, morphological analysis, abrasive grains, Abral®

INTRODUCTION

The development of modern abrasive machining processes is most often associated with:

- the introduction of new construction materials, challenging the abrasive tools through their hard-to cut properties;
- development of new kinematic varieties of the grinding process;
- the introduction of new abrasive materials.

Significant progress in the field of new abrasives hasn't occurred since the 1980s, when the company 3M (1981) and later Norton (1986) presented a new type of microcrystalline sintered corundum grain, obtained through the sol-gel process. It took till 2000 for French company Pechiney Electrometallurgie Abrasives & Refractories to devise and implement the technology that enabled the production of alumina oxynitride abrasive grains.

The γ-alumina oxynitride (AlxOyNz - in brief AlON) is known as a ceramic material used in the production of semiconductor substrates for the electronics industry, among other things. As an abrasive material it was first used in 1980 [1]. AlON grains production technology consisted of creating a fine-grained mixture of solid precursor (Al_2O_3 and AlN), developing their heat treatment in an oxidizing environment, and in the final sintering process, being compacted to a value of at least 97% of the theoretical density. This was meant to create a regular form of alumina oxynitride spinel. In 1988 [2] and then in 1990 [3] 3M company developed and patented production technology of abrasives made from Al_2O_3, γ variety alumina oxynitride and nitride culled from the group IVb metals of the Periodic Table. In this case, the abrasives production method was based upon the sol-gel process and the reactive sintering technique. In 1991, the company Pechiney Electrometallurgie patented the process of direct nitriding of metals with a

relatively low melting point, particularly for aluminum [4]. The same company in 1991, developed a wide range of abrasives and refractory materials based on oxynitrides, including materials with type AlON alumina oxynitride, obtained through direct nitriding, electric furnace melting and rapid cooling of the molten material [5]. This enabled a significant reduction in the manufacturing cost of this type of abrasive material that was characterized by an equivalent AlN content of from 11% to 12.5%. The next step in the development of AlON grain production technology was in 1995, when Pechiney Electrometallurgie developed abrasives based on oxynitride AlON obtained by sintering in an electric furnace whose hardness was increased due to the dispersion of fine-grained crystals of titanium carbide in the base material [6].

Based on technology developed in 2000, the company Pechiney Electrometallurgie Abrasives & Refractories started production of alumina oxynitride abrasive grains under the trademark Abral® for abrasive tools with vitrified and resin bond for precision and highly efficient grinding processes [7].

The French company Pechiney Electrometallurgie were acquired by the Canadian Alcan Inc. in 2003, becoming Pechiney International SA. However, in October 2007, Alcan Inc. was bought by Rio Tinto, one of the leading mining companies [8, 9]. The combination of the existing structures of Rio Tinto, involved in the extraction and processing of Aluminum, with resources of Alcan Inc, led to the founding of Rio Tinto Alcan, which In turn transformed into a Company called Alteo, manufacturing the Abral® abrasive grains in one of its factories in La Bâthie in France [10, 11].

Table 1. The chemical composition and properties of the types of abrasive grain analyzed [12-17]

	White fused alumina 99A	**Microcrystalline sintered corundum**	**Silicon carbide 99C**	**cBN**	**Abral®**
Full name	fused alumina Al_2O_3	Microcrystalline sol-gel sintered alumina	silicon carbide green SiCg	cubic boron nitride cBN	aluminium oxynitride $Al_xO_yN_z$
Chemical composition	Al_2O_3: 99.7% SiO_2: 0.01% Fe_2O_3: 0.02% Na_2O: 0.16% CaO+MgO:0.02%	Al_2O_3: 95-99% MgO/Fe_2O_3: 0-5%	>98.5% SiC ~0.30% C ~0.02% Fe ~0.03% Si	~43.6% B ~56.4% N	$Al_xO_yN_z$: 99.5% SiO_2: 0.06% Fe_2O_3: 0.03% Na_2O: 0.11%
Crystal size	~10 μm	< 1 μm	< 1 μm	from ~10 μm (monocrystalline) to < 1 μm (microcrystalline)	~10 μm
Shape	pointed, sharp	pointed, very sharp	sharp, angular	block (hexagonal) or irregular, very sharp	pointed, very sharp
Specific density	3.96 g/cm^3	3.87 g/cm^3	3.12-3.21 g/cm^3	3.48 g/cm^3	3.65 g/cm^3
Knoop hardness HK	20.3 GPa	21.5 GPa	24-30 GPa	42-54 GPa	18.0 GPa
Ductility	2.0 MPa• m $^{1/2}$	3.7 MPa• m $^{1/2}$	2.2-3.3 MPa• m$^{1/2}$	-	1.65 MPa• m $^{1/2}$
The critical stress intensity factor K_{Ic}	2.7 MPa• m $^{1/2}$	3.5-4.3 MPa• m $^{1/2}$	1.9 MPa• m $^{1/2}$	3.7 MPa• m $^{1/2}$	-
Coefficient of friction (hardened steel)	0.34	0.19	-	0.19	-
Thermal conductivity coefficient λ	27-35 W/m•K	27-35 W/m•K	3.2-4.9 W/m•K	240-1300 W/m•K	-

Alumina oxynitride abrasive grains have a polycrystalline structure, and a slightly lower hardness and toughness compared with white fused alumina 99A. Table 1 contains a summary of the most important properties of the AlON abrasive grains, with respect to the grains of Al_2O_3, SiC and cBN.

The morphological characteristics of the abrasive grains are extremely important for modeling and simulation of abrasive machining processes, among others [18-21]. Most of the modeling methods described in the literature assumes an approximate functioning description of abrasive grain geometry. Increasingly, however, advanced model of cutting vertices geometry are being applied in order to increase the reliability and accuracy of the results obtained from the simulation of the machining processes implemented using such models. Therefore, when a new generation of abrasive grains is introduced, it is necessary to develop new geometric models reflecting the essential morphological characteristics of such grains. The aim of this article is to characterize the geometrical features of AlON abrasive grains in comparison to other commonly used abrasives with Al_2O_3 (white fused alumina 99A and microcrystalline sintered corundum SG), green SiC (99C) as well as mono- and microcrystalline cubic boron nitride (cBN).

MATERIALS AND METHODS

The main goal of the experimental investigations

The aim of this study was to analyze the morphology of the new generation abrasive grains AlON, particularly with respect to the most commonly used abrasive grains: Al2O3, SiC and cBN. This analysis was conducted using scanning electron microscopy and associated methods of computer image processing and analysis.

Sample characteristics and preparation

Six types of abrasive grains were examined: 99A, SG, 99C, cBN (mono- and microcrystalline), as well as Abral ®, characterized in Table 1. The abrasive grains analyzed numbered F46 to F80. These numbers determine the abrasive grains characteristic dimensions according to FEPA standards [22]. Before the acquisition process all types of abrasive grains were prepared and placed upon the specimen stage. Then a common procedure was utilized in which the surfaces of all the samples were cleaned by compressed air. In order to obtain a higher than standard contrast of the image surface of the grains, some of them (SiC and AlON (Abral®) were placed upon carbon adhesive tape. The grains selected for acquisition were subjected to an additional treatment (eg. coating, washing, etc.).

Observation and acquisition of the SEM micrographs

In the studies presented to assess the morphology of the samples, scanning electron microscopy was used [23-25]. Acquisition of the micrographs was carried out using the scanning electron microscope JSM-5500LV by JEOL Ltd. (Japan) [23, 24]. The instrument was equipped with two types of detector - secondary electron image (SEI) and backscattered electron detector (BEI) which operated in two modes: high vacuum mode (HVM) and low vacuum mode (LVM). In HVM the producer guaranteed a resolution (SEI) 4.0 nm (AV=30 kV, WD=6 mm) and mag. from 18 to 300000 (realized in 36 steps). The resolution (BEI) for LVM was 5.0 nm (AV=30 kV, WD=8 mm) at an adjustable pressure of 10 to 270 Pa. Evacuation time for HVM was approx. 100 s, whereas for LVM approx. 90 s. The electron gun used an AV from 0.5 to 30 kV (53 steps). An eucentric goniometer type specimen stage was able to carry out the movement in the direction x (20 mm), y (10 mm) and z (43 mm) axes. The maximal sample size, which could be put on the table was 152.4 mm.

The acquisition was carried out mainly through the use of a BEI detector. A wide range of mags. were used from 25x (general morphology of a group of the abrasive grains) to 1700x (details of the area of interest (AOI) of the selected abrasive grains) with an AV from 8 to 20 kV,

and a vacuum pressure of 1-9 Pa. The acquired micrographs were characterized by the following parameters: resolution 1280x960 pixels, 8-bit color depth, greyscale mode, saving format *.bmp.

In Fig. 1 the general view of the scanning electron microscope JSM-5500LV by JEOL Ltd., which was used in the experimental investigations, is presented.

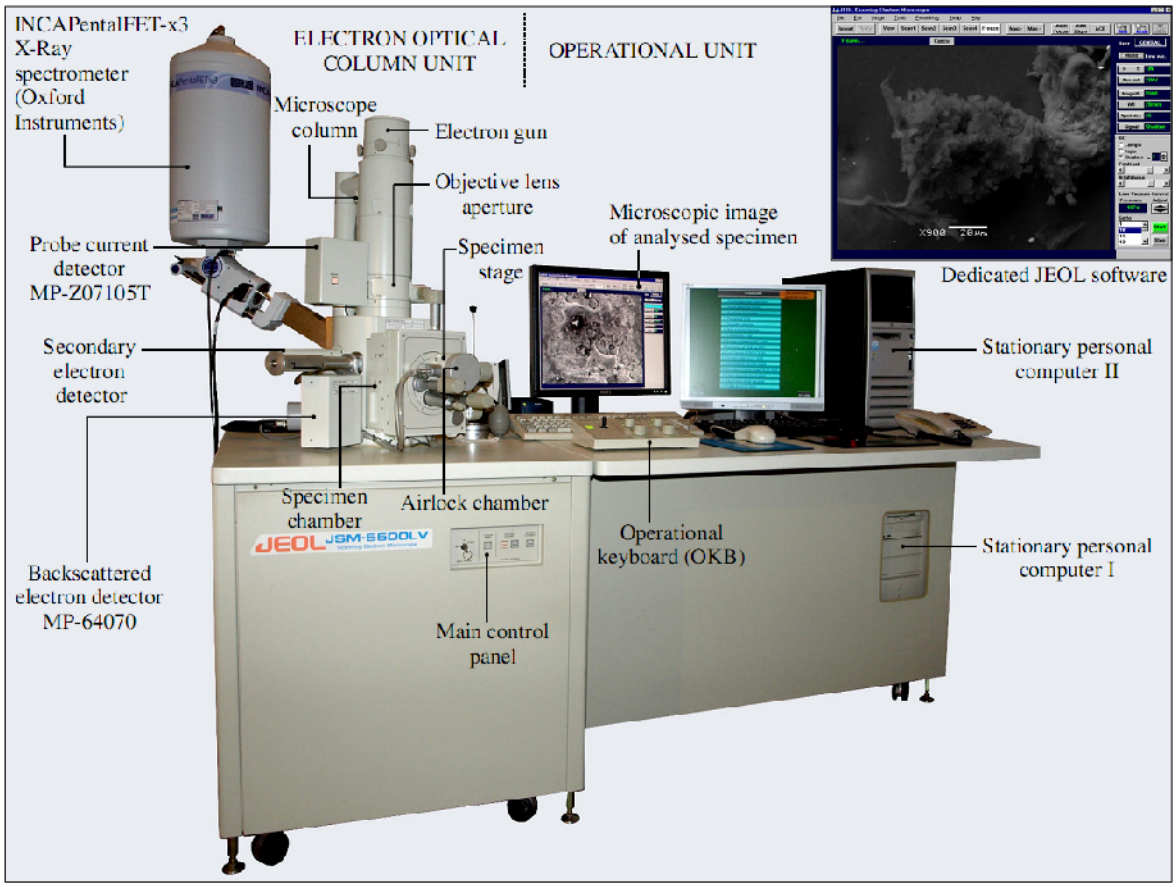

Fig. 1. General view of scanning electron microscope JSM-5500LV by JEOL Ltd. (Japan) used in the experimental investigations. The microscopy system was additionally equipped with a dispersive spectrometer module INCAPentaFET-x3 with Si(Li) detector by Oxford Instruments (Great Britain).

Morphological analysis of the SEM micrographs

Morphological analysis often comes down to the definition of some geometrical quantities characterizing the test object. In the case presented in this paper, the authors restricted themselves to carrying out basic geometrical measurements of the abrasive grains. Although this analysis is fundamentally a very simplified one, it enables the general analysis of all types of abrasive grain. The combination of a morphological analysis of visual observation enables the extraction of multiple geometric features (described quantitatively and qualitatively) of the different abrasive grains evaluated. The combination of the morphological analysis and visual observation also enables the detailing of many geometric features (described in quantitative and qualitative fashion), which differ in terms of the abrasive grain.

The measurements of all abrasive grains were carried out using Image-Pro® Plus 5.1 software created by Media Cybernetics Inc. (USA). The main goal of this study was to determine the geometrical dimensions of the individual grains in the acquired SEM micrographs. The measurement procedure consisted of loading the SEM

micrograph image, extracting the single grain form from the image, removing all backgrounds, binarization and and, finally, calculation (in automatic mode) of the values of the two parameters which characterized the abrasive grain geometry. These were:

- Feret (max) longest caliper (feret) length,
- Feret (min) smallest caliper (feret) length.

Additionally, by using the function *Measurements* the values of the apex angle were calculated (in manual mode). All of the above parameters were determined for 30 randomly selected abrasive grains.

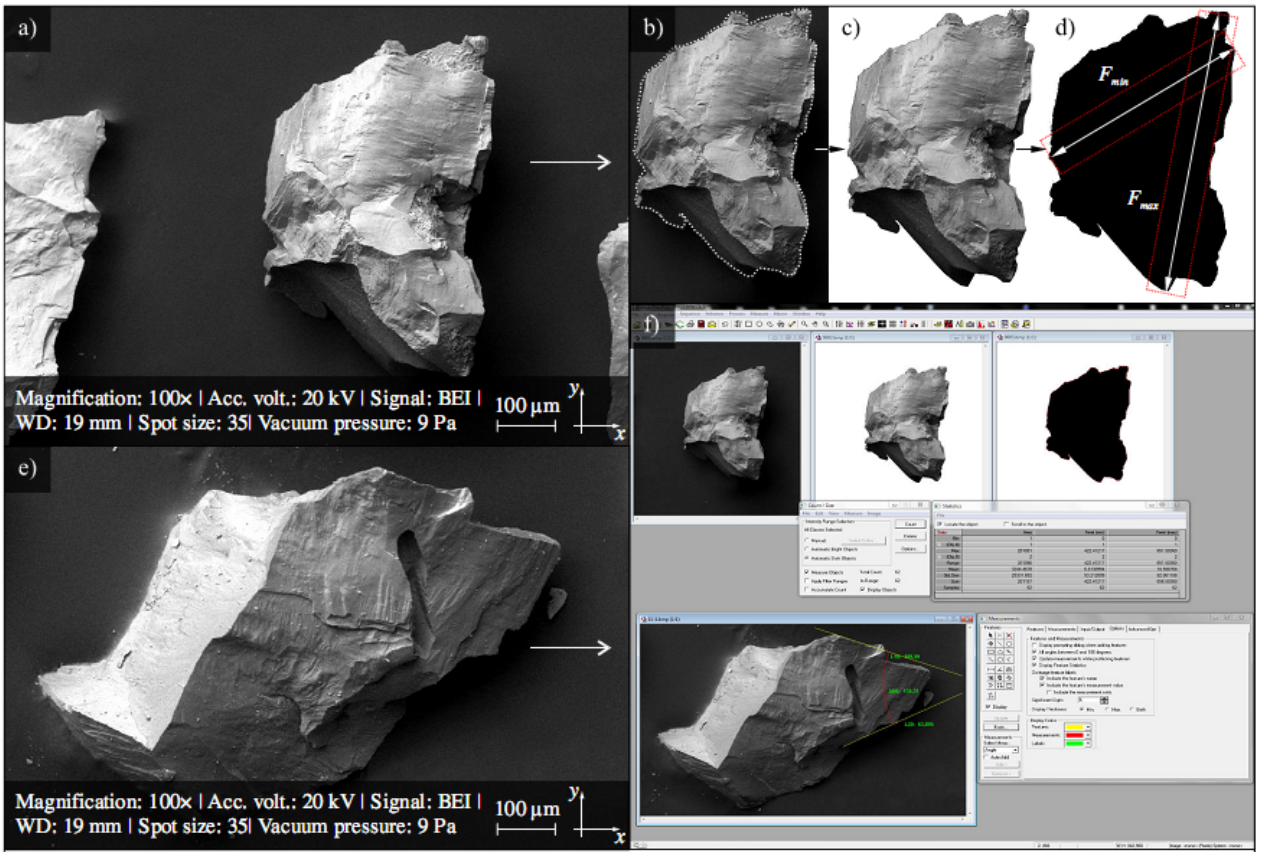

g) Average values of parameters

Grain type		Parameter			Grain type		Parameter		
		F_{max}, mm	F_{min}, mm	Apex angle, °			F_{max}, mm	F_{min}, mm	Apex angle, °
SG™	F46	0.60	0.32	151.20	99A	F46	0.53	0.32	132.08
	F60	0.48	0.24	140.28		F60	0.42	0.22	120.26
	F80	0.32	0.11	156.26		F80	0.31	0.17	124.58
SiC	F46	0.58	0.42	157.33	cBN	mono	0.16	0.09	110.47
AlON	F46	0.61	0.36	133.07		micro	0.06	0.03	120.42

Fig. 2. The following steps were carried out during the determination of the basic geometrical parameters of the abrasive grains by using Image-Pro® Plus 5.1 software: a) input micrograph (AlON grain, 1.05x0.80 mm, mag. 100x), b) extraction of a single grain, c) extraction of background, d) the binarization process and the idea of determining Maximum (F max) and Minimum (F min) Feret diameter, e) input micrograph (AlON grain, 0.69x0.15 mm, mag. 100x), f) the above procedure realized through the Image Pro® Plus 5.1 software in automatic (F max, F min) and manual (apex angles) mode, g) the calculated average values of parameters.

In Fig. 2 the steps conducted during processing and analysis of the abrasive grains SEM micrographs are presented.

RESULTS AND DISCUSSION

Among the study group of grains clearly distinct morphology emerged, characterized by monocrystalline cBN grains, which have a shape similar to a regular octahedron (Fig. 3). These grains are further characterized by a conchoidal fracture. In the accompanying microscopic images even the smallest characteristic features of the grains with monocrystalline structure can be observed. Cracks propagate in them without finding the intergranular boundaries, causing chipping of large portions of the grain. Examples of such cracks can be observed in Fig. 3d and Fig. 3f.

Both the a second type of cBN grains (Fig. 4) and SG^{TM} grains (Fig. 5) have microcrystalline structure. They consist of crystallites of a size <1 μm, which means that they have a very developed surface. Also, a fracture quality of these grains significantly differentiates them from other types. This difference is due to the different mechanism of destruction. The energy used to crack in microcrystalline grains is dispersed through a number of crystals boundaries so that its propagation is suppressed. In effect much smaller fragments of grains are crumbled out than is the case with poly- and monocrystalline grains. It should be noted, however, that the tested microcrystalline sintered corundum grains (SG) are characterized by a much more flattened shape than microcrystalline cBN grains and other types of grain. The closest crystalline structures have grains of white fused alumina 99A (Al_2O_3), 99C (SiC) and Abral ® (AlON). A similar morphology within AlON (Figs. 6 and 7) and SiC (Fig. 8) grains is likely due to their similar manner of cracking, in which the cracks propagate along the borders of the polycrystals. Also, both grains share similar crystallite size (~10 μm). Green silicon carbide grains have a conchoidal fracture (Fig. 8b and Fig. 8c).

In characterizing the morphology of a new generation of AlON grains (Figs. 6 and 7), on the basis of the recorded SEM images and measurements of geometrical quantities, it can be concluded that these grains are to a large extent similar to white fused alumina 99A grains (Fig. 9). This becomes apparent in particular features, such as their polycrystalline structure, pointed shape, developed surface and similar apex angle values (Fig. 2g). Therefore, in the case of modeling the microgeometry of abrasive tool active surfaces made from Abral® there should already be adequate models developed for white fused alumina grains.

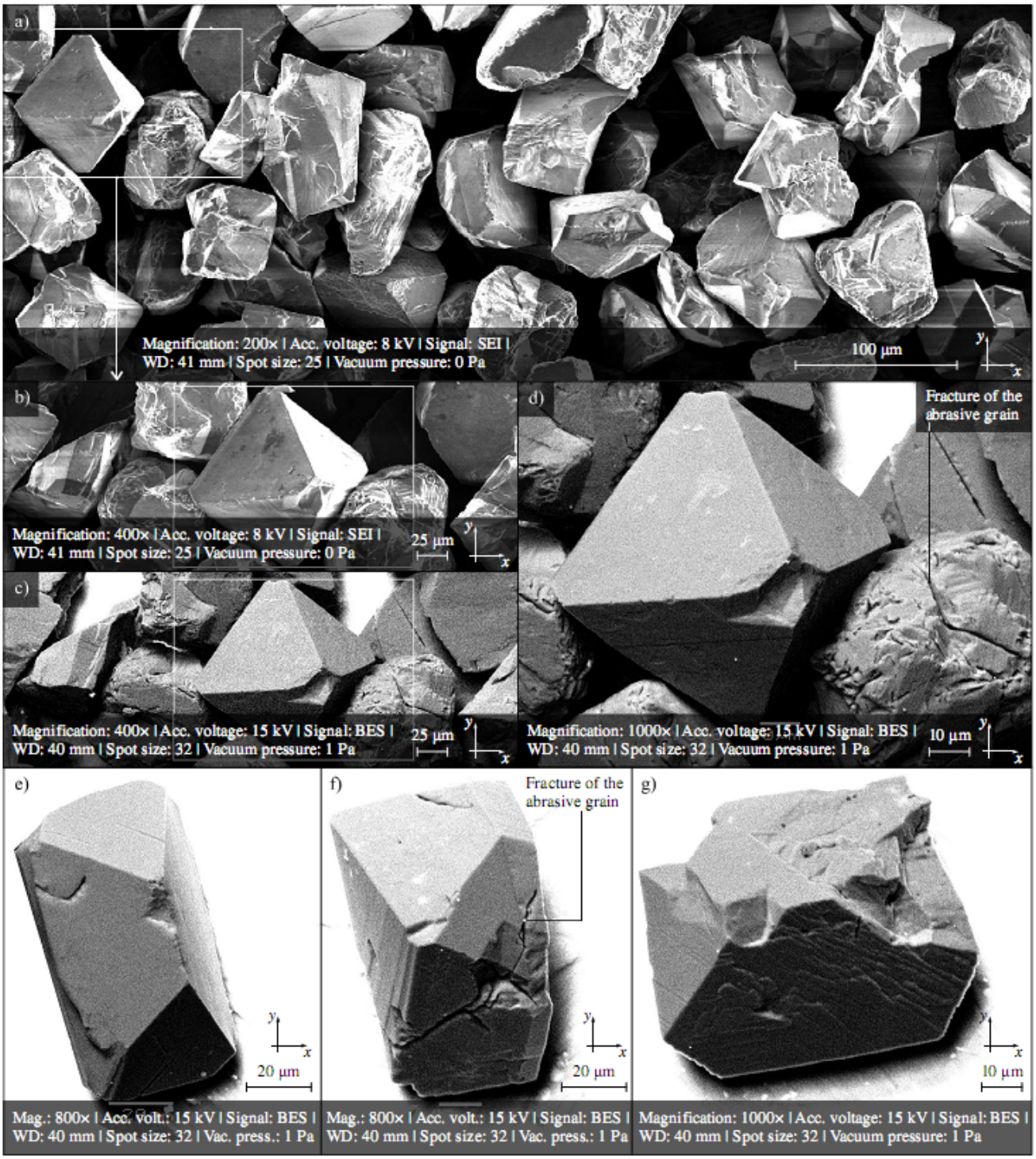

Fig. 3. General morphology of the abrasive grains cBN (monocrystalline) obtained by use of scanning electron microscope JSM-550LV produced by JEOL: a) SEM micrograph presenting a vast panorama (0.65x0.23 mm, mag. 100x) of the abrasive grains cBN, b),c) AOI (0.32x0. 11 mm, mag. 400x) extracted from Fig. 3a, d) AOI (0.12x 0.009 mm, mag. 1000x) extracted from Fig. 3c, e)-g) SEM micrograph (mag. 800-1000x) of a single abrasive grain of cBN.

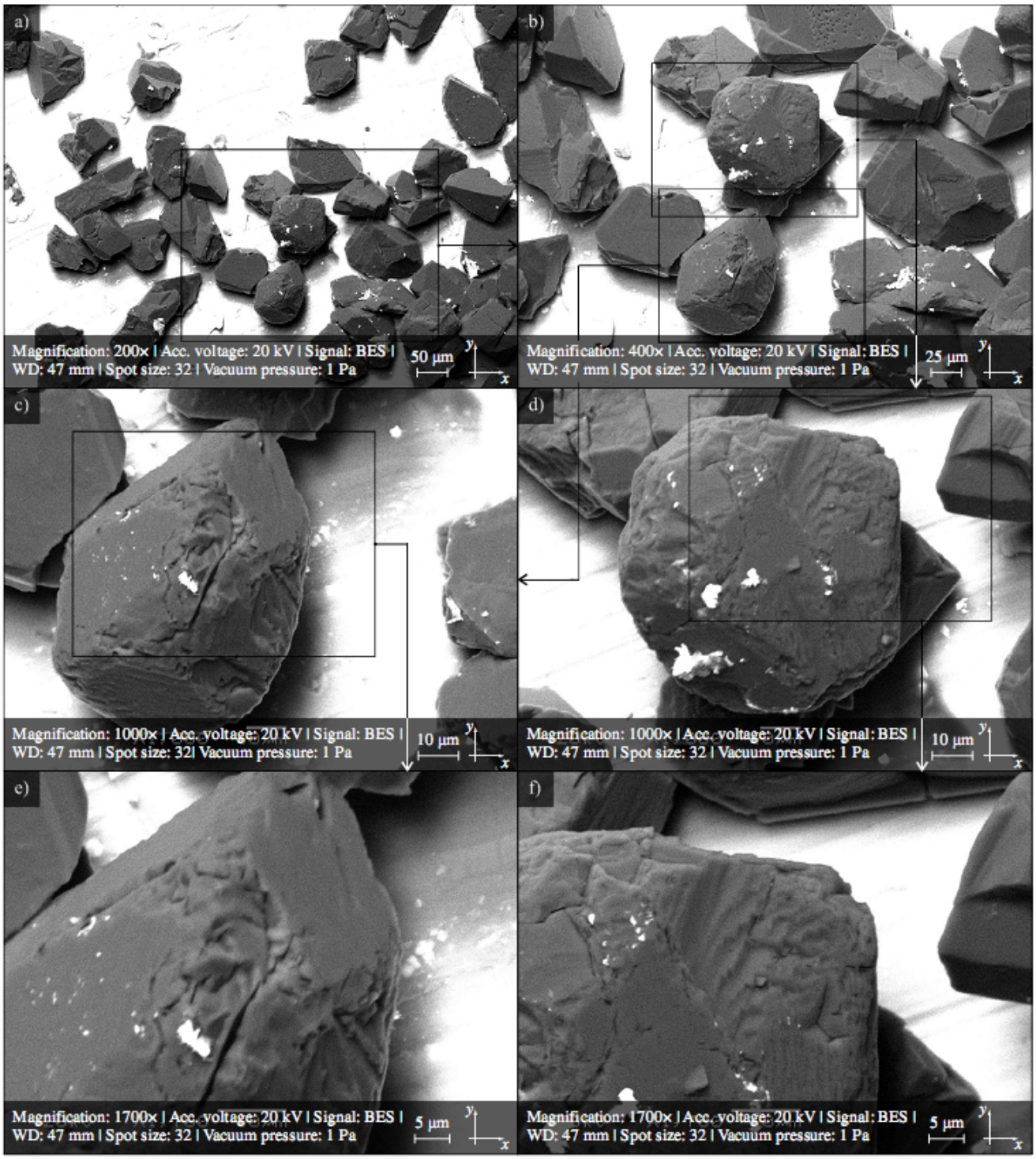

Fig. 4. General morphology of the abrasive grains cBN (microcrystalline) obtained by use of scanning electron microscope JSM-550LV produced by JEOL: a) SEM micrograph (0.74x0.54 mm, mag. 200x) of a group of the abrasive grains cBN, b) AOI (0.37x0.27 mm, mag. 400x) extracted from Fig. 4a, c), e) AOIs (0.013x0.010 mm, mag. 1000x) extracted from Fig. 4b, d), f) AOIs (0.013x0.010 mm, mag. 1000x) extracted from Fig. 4b, d), f) AOIs (0.072x0.054 mm, mag. 1700x) extracted (respectively) from Fig. 4c and Fig. 4e

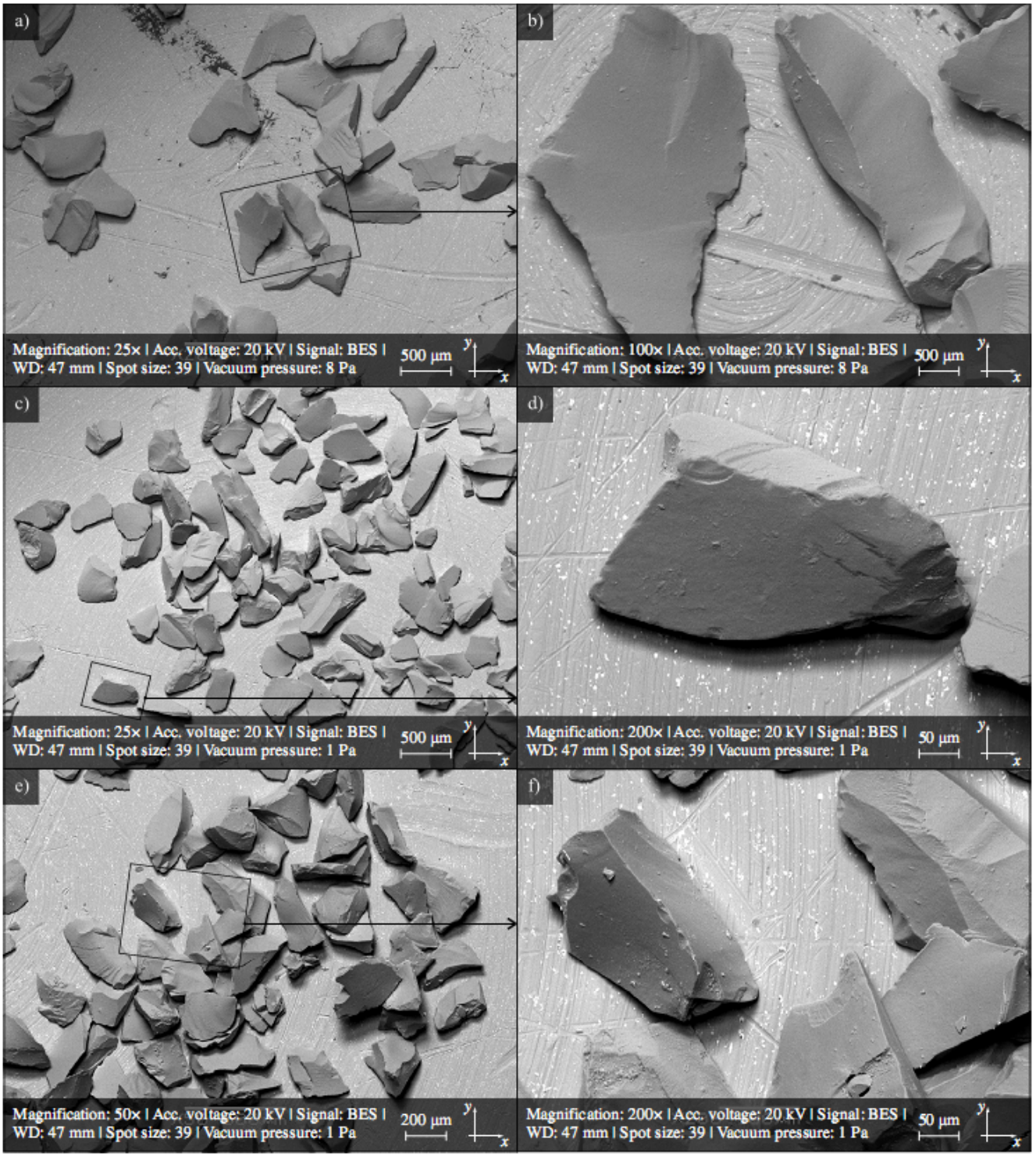

Fig. 5. General morphology of the abrasive grains SG^{TM} obtained by use of scanning electron microscope JSM-550LV produced by JEOL: a) SEM micrograph (5.08x3.81 mm, mag. 25x) of a group of the abrasive grains SG^{TM} 46, b) AOI (0.13x0.09 mm, mag. 100x) extracted from Fig. 5a, c) SEM micrograph (5.08x3.81 mm, mag. 25x) of a group of the abrasive grains SG^{TM} 60, d) AOI (0.06x0.04 mm, mag. 200x) extracted from Fig. 5c, e) SEM micrograph (2.54x1.90 mm, mag. 50x) of a group of the abrasive grains SG^{TM} 80, f) AOI (0.64x0.48 mm, mag. 200x) extracted from Fig. 5e.

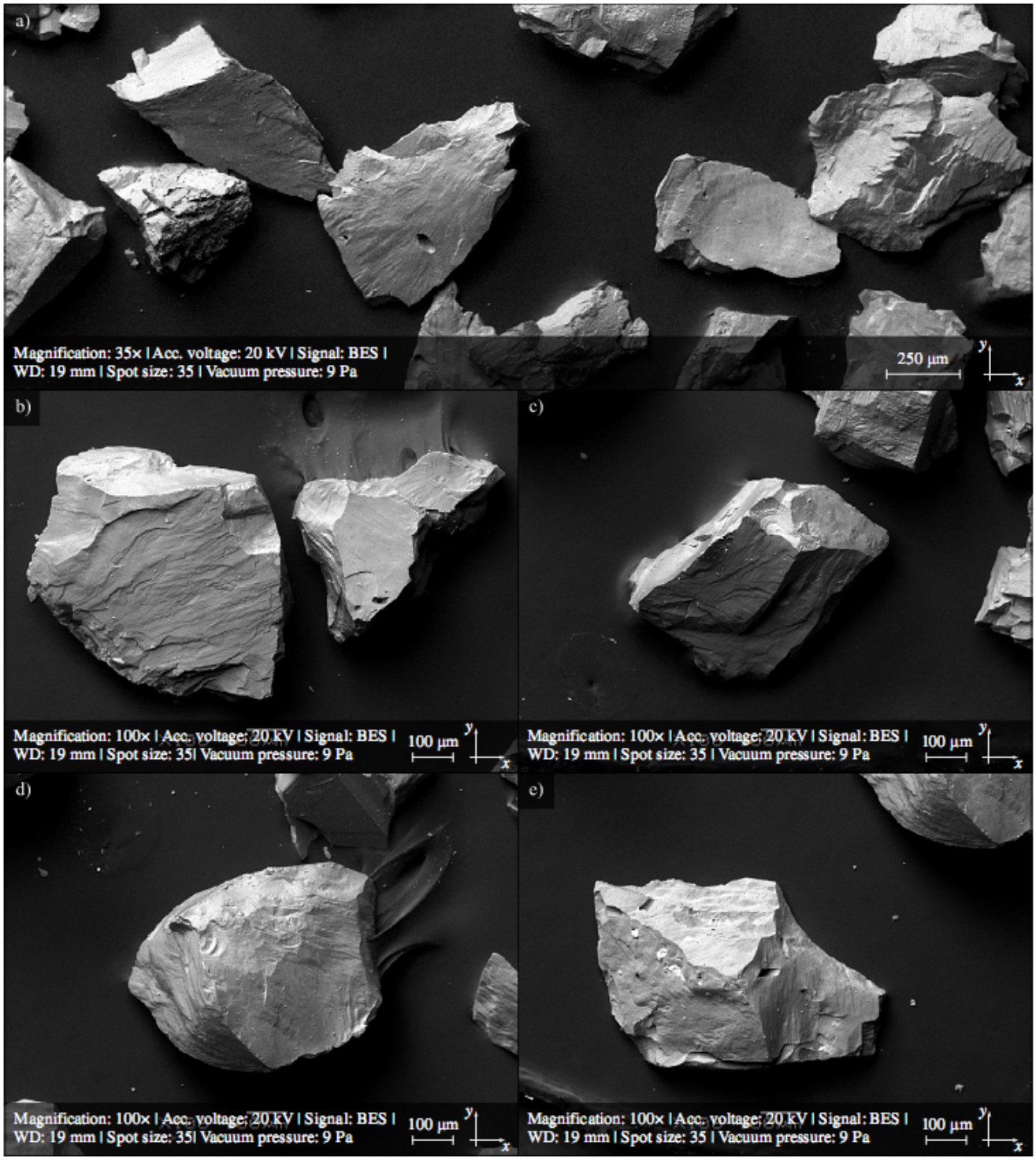

Fig. 6. General morphology of the AlON-based abrasive grains (Abral®) obtained by use of scanning electron microscope JSM-550LV produced by JEOL: a) SEM micrograph presenting a vast panorama (3.5x1.31 mm, mag. 135x) of the abrasive grains AlON (Abral®), b)-e) SEM micrograph (1.25x0.93 mm, mag. 100x) of a single abrasive grain AlON (Abral®).

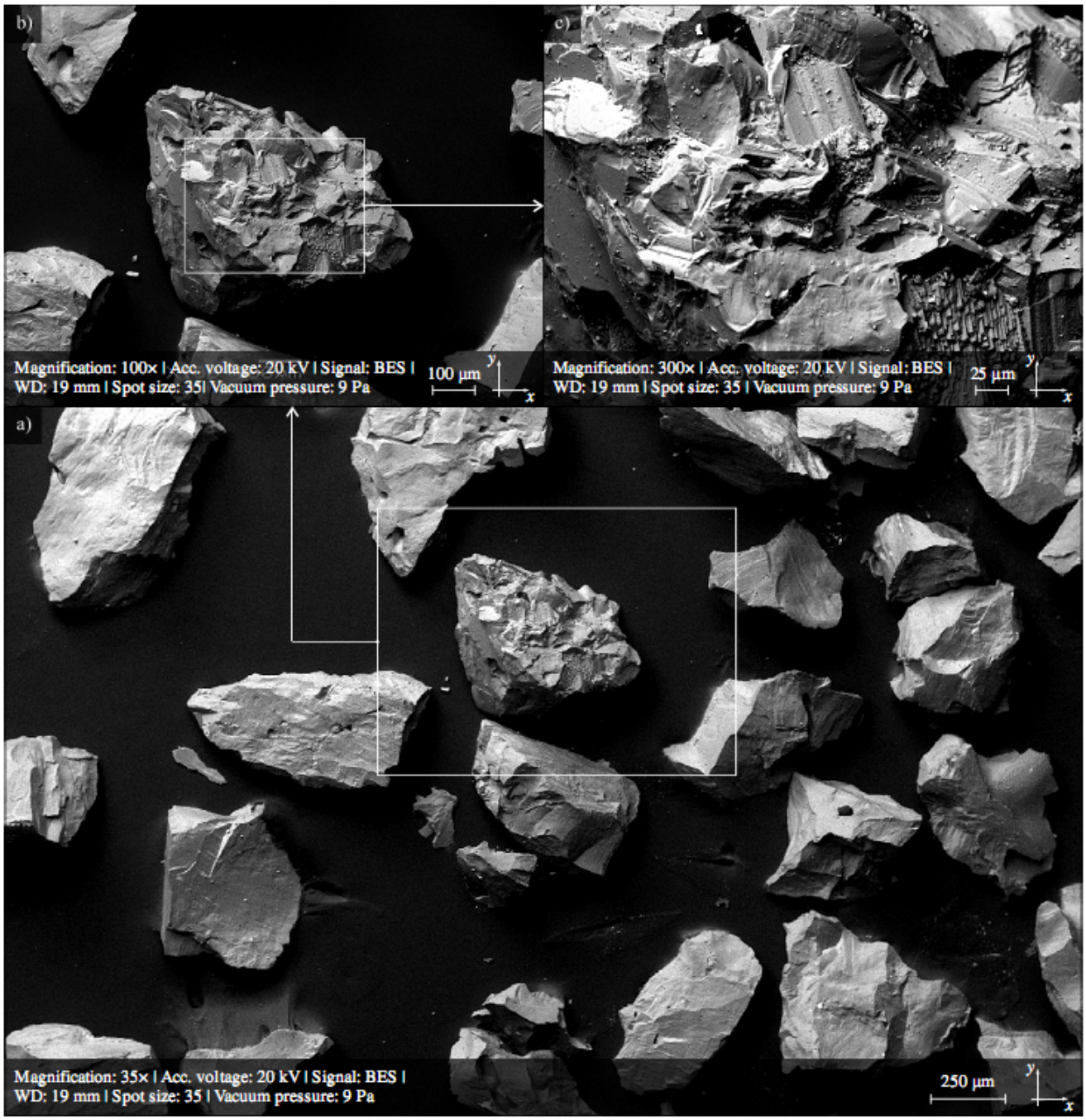

Fig. 7. Details of the fracture morphology of the AlON-based abrasive grains (Abral®) obtained by use of scanning electron microscope JSM-550LV produced by JEOL: a) SEM micrograph presenting a vast panorama (3.63x2.71 mm, mag. 35x) of the abrasive grains AlON (Abral®), b) AOI (1.28x0.96 mm, mag. 100x) extracted from Fig. 7a, c) AOI (0.42x0.31 mm, mag. 300x) extracted from Fig. 7b.

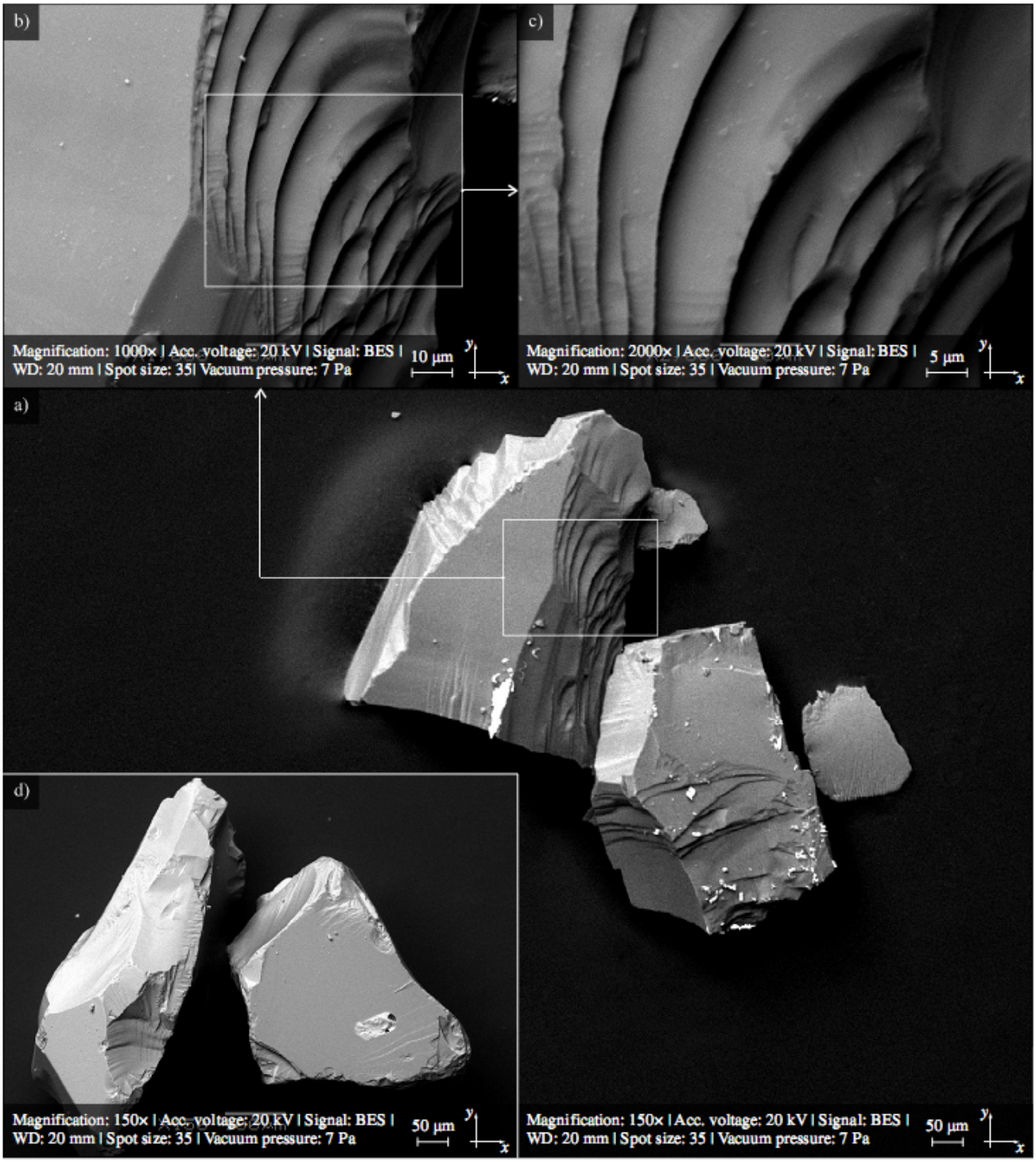

Fig. 8. General morphology of the abrasive grains SiC obtained by use of scanning electron microscope JSM-550LV produced by JEOL: a) SEM micrograph (0.83x0.62 mm, mag. 150x) of the abrasive grains SiC, b) AOI (0.12x0.09 mm, mag. 1000x). Extracted from Fig. 8a, c) AOI (0.06x0.04 mm, mag. 2000x) extracted from Fig. 8b, d) SEM micrograph (0.83x0.62 mm, mag. 150x) of a single abrasive grain SiC.

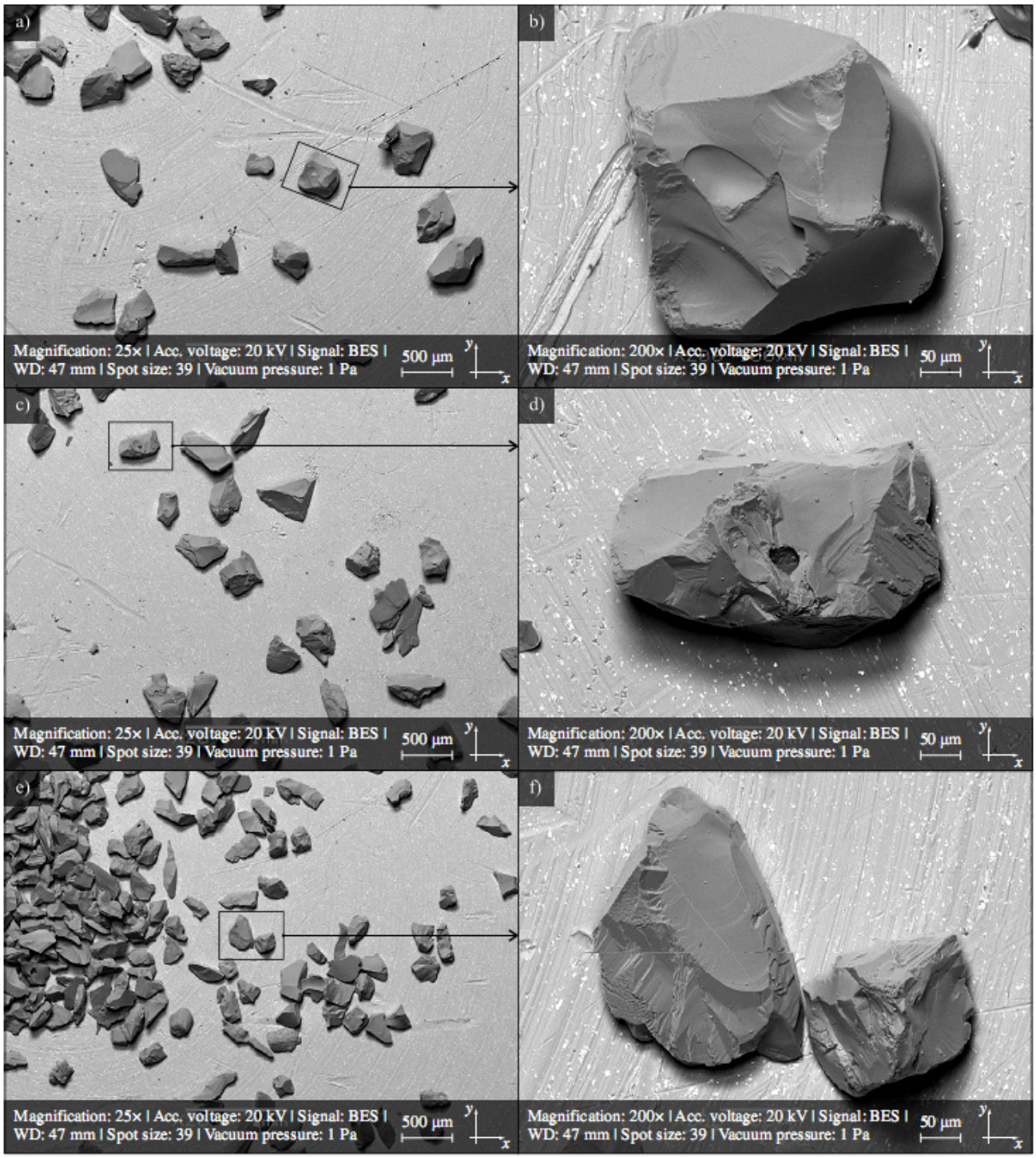

Fig. 9. General morphology of the abrasive grains 99A obtained by use of scanning electron microscope JSM-550LV produced by JEOL: a) SEM micrograph (5.08x3.81 mm, mag. 25x) of a group of the abrasive grains 99A 46, b) AOI (0.64x0.48 mm, mag. 200x) extracted from Fig. 9a, c) SEM micrograph (5.08x3.81 mm, mag. 25x) of a group of the abrasive grains 99A 60, d) AOI (0.64 x0.48 mm, mag. 200x) extracted from Fig. 9c, e) SEM micrograph (5.08x3.81 mm, mag. 25x) of a group of the abrasive grains 99A 80, f) AOI (0.64x0.48 mm, mag. 200x) extracted from Fig. 9e.

CONCLUSIONS

The results presented of the morphological analysis of the Abral® abrasive grains compared to other kinds of grains studied, led to the following conclusions:

- AlON grains have many features similar to white fused alumina 99A grains, such as: polycrystalline structure, pointed shape, developed surface and close apex angle values;
- The microgeometry of fractures in the AlON and 99A grains are very similar; this probably results from the analogous manner of the cracking, in which the cracks propagate along the borders of the polycrystals, as well as the fact that the two kinds of grains have similar sized crystallites (~10 μm), but this should be confirmed by additional studies;
- A similar morphology of Abral® and 99A abrasive grains enables the drawing of a conclusion that in a variety of applications the geometric models developed for 99A grains should adequately characterize the new generation of AlON grains;
- the analysis of the geometry of the abrasive grains using scanning electron microscopy imaging methods, supported by computer image processing and analysis, allows for multi-criteria morphological assessment of these objects in microscale.

ACKNOWLEDGEMENTS

The Authors wish to thank Mr. Ryszard Gritzman and Zbigniew Kuklinski, MSc, BSc, from the Laboratory of Electron Microscopy and the Structural Research Central Laboratory of the Institute of Mechatronics, Nanotechnology and Vacuum Technique at Koszalin University of Technology (Poland), for acquisition of SEM micrographs by JSM-5500 LV. The Authors would especially like to thank the Rio Tinto Alcan company for providing the Abral® abrasive grains for the research.

REFERENCES

[1] McCauley J.W., Corbin N.D. (1980) Process for Producing Polycrystalline Cubic Aluminum Oxynitride US Patent No. 4241000.

[2] Mathers J.P., Wood W.P. (1988) Aluminum Nitride/Sluminum Oxynitride/Group IVB Metal Nitride Abrasive Particles derived from a Sol-gel Process US Patent No. 4788167.

[3] Mathers J.P., Wood W.P., Forester T.E. (1990) Aluminum Oxide/Aluminum Oxynitride/Group IVB Metal Nitride Abrasive US Particles derived from a Sol-Gel Process Patent No. 4957886.

[4] Dubots D., Faure P. (1994) Process for Direct Nitriding of Metals of Low Melting Point US Patent No. 5314675.

[5] Dubots D., Faure P. (1994) Abrasive and/or Refractory Products based on Melted and Solidified Oxynitrides and Process Preparing the Same US Patent No. 5336280.

[6] Galvin H.P. (1995) Abrasive material France Patent FR2720391.

[7] Ceramic Industry (2000) Whats New in Abrasives, http://www.ceramicindustry.com/articles/875 34-what-s-new-in-abrasives.

[8] Our History (2014), Rio Tinto Alcan, http:// www.riotintoalcan.com/ENG/whoweare/28.asp

[9] Corporate profile (2013), Rio Tinto Fact Sheet, http://www.riotinto.com/documents/Reports_Publications/corpPub_Corporate.fr.pdf

[10] History (2014), Rio Tinto, http://www.riotinto.com/aboutus/history-4705.aspx.

[11] La Bâthie (2014), Alteo. at: http://alteoalumina.com/en/la-b%C3%A2thie

[12] MSDS Alteo Abral REACH eng 20130814 (2014), Alteo, http://alteo-alumina.com/en/resources.

[13] Bourlier F. (2005) Abrasive Particles based on Aluminium Oxynitride US Patent Application Publication No. 2005/0160678 A1.

[14] Klocke F. (2009) Manufacturing Processes 2: Grinding, Honing, Lapping Berlin, Springer.

[15] Rowe W.B. (2009) Principles of Modern Grinding Technology Burlington, William Andrew.

[16] Jackson M.J., Davim J.P. (2010) Machining with Abrasives New York, Springer.

[17] Gerhardt R. (2011) Properties and Applications of Silicon Carbide Rijeka, Intech.

[18] Brinksmeier E., Aurich J.C., Govekar E., Heinzel C., Hoffmeister H.-W., Klocke F., Peters J., Rentsch R., Stephenson D.J., Uhlmann E., Weinert K., Wittmann M. (2006) Advances in Modeling and Simulation of Grinding Processes. *CIRP Ann*. 55:667-696.

[19] Jiang J.L., Ge P.Q., Bi W.B., Zhang L., Wang D.X., Zhang Y. (2013) 2D/3D Ground Surface Topography Modeling Considering Dressing and Wear Effects in Grinding Process. *Int. J. Mach. Tools Manuf.* 74:29-40.

[20] Liu Y., Warkentin A., Bauer R., Gong Y. (2013) Investigation of Different Grain Shapes and Dressing to Predict Surface Roughness in Grinding Using Kinematic Simulations. *Precis. Eng*. 37:758-764.

[21] Zhu D., Yan S., Li B. (2014) Single-Grit Modeling and Simulation of Crack Initiation and Propagation in SiC Grinding Using Maximum Undeformed Chip Thickness. *Comput. Mater. Sci*. 92:13-21.

[22] FEPA-Standard 42-1:2006 (2006) Grains of Fused Aluminium Oxide, Silicon Carbide and Other Abrasive Materials for Bonded Abrasives and for General Applications. *Macrogrits* F 4 to F 220.

[23] Kaplonek W., Nadolny K. (2012) Review of the Advanced Microscopy Techniques Used for Diagnostics of Grinding Wheels with Ceramic Bond. *Journal of Machine Engineering* 12(4):8198.

[24] Kaplonek W., Nadolny K. (2013) Assessment of the Grinding Wheel Active Surface Condition using SEM and Image Analysis Techniques. *J. Braz. Soc. Mech. Sci. Eng.* 35(3):207-215.

[25] Kaplonek W., Nadolny K. (2013) Advanced Desktop SEM Used for Measurement and Analysis of the Abrasive Tools Active Surface. *Acta Microsc*. 22(3):278-288.